Multifractal characteristics and spatial variability of soil particle-size distribution in different land use patterns in a small catchment of the Three Gorges Reservoir Region, China

Tai-li CHEN, Zhong-lin SHI, An-bang WEN, Dong-chun YAN, Jin GUO, Jia-cun CHEN, Yuan LIU, Rui-yin CHEN

Original Article

Multifractal characteristics and spatial variability of soil particle-size distribution in different land use patterns in a small catchment of the Three Gorges Reservoir Region, China

CHEN Tai-li[1,2] https://orcid.org/0000-0001-5027-8885; e-mail: chentaili1994@126.com

SHI Zhong-lin[1] https://orcid.org/0000-0003-0169-5062; e-mail: shizl@imde.ac.cn

WEN An-bang[1] https://orcid.org/0000-0001-6852-7464; e-mail: wabang@imde.ac.cn

YAN Dong-chun[1*] https://orcid.org/0000-0002-9130-5410; ✉ e-mail: yandc@imde.ac.cn

GUO Jin[3] https://orcid.org/0000-0003-0249-0421; e-mail: 498406643@qq.com

CHEN Jia-cun[1,2] https://orcid.org/0000-0002-8407-3746; e-mail: 532305479@qq.com

LIU Yuan[1,2] https://orcid.org/0000-0003-0524-2968; e-mail: 306liuyuan@163.com

CHEN Rui-yin[1,2] https://orcid.org/0000-0002-9987-6082; e-mail: chenruiyin@imde.ac.cn

* Corresponding author

1 *Key Laboratory of Mountain Surface Processes and Ecological Regulation, Institute of Mountain Hazards and Environment, Chinese Academy of Sciences, Chengdu 610041, China*

2 *University of Chinese Academy of Sciences, Beijing 100049, China*

3 *Department of Resources and Environmental Engineering, Sichuan Water Conservancy Vocational College, Chengdu 611231, China*

Abstract: Characterizing soil particle-size distribution is a key measure towards soil property. The purpose of this study was to evaluate the multifractal characteristics of soil particle-size distribution among different land-use from a purple soil catchment and to generalize the spatial variation trend of multifractal parameters across the catchment. A total of 84 soil samples were collected from four kinds of land use patterns (dry land, orchard, paddy, and forest) in an agricultural catchment in the Three Gorges Reservoir Region, China. The multifractal analysis method was applied to quantitatively characterize the soil particle size distribution. Six soil particle size distribution (PSD) multifractal parameters ($D(0)$, $D(1)$, $D(2)$, $\Delta\alpha(q)$, $\Delta f[\alpha(q)]$, $\alpha(0)$) were computed. Additionally, a geostatistical analysis was employed to reveal the spatial differentiation and map the spatial distribution of these parameters. Evident multifractal characteristics were found. The trend of generalized dimension spectrum of four land use patterns was basically consistent with the range of

0.8 to 2.0. However, orchard showed the largest monotonic decline, while the forest demonstrated the smallest decrease. $D(0)$ of the four land use patterns were ranked as: dry land < orchard < forest < paddy, the order of $D(1)$ was: dry land < paddy < orchard < forest, $D(2)$ presented a rand-size relationship as dry land < forest < paddy < orchard. Furthermore, all land-use patterns presented as $\Delta f[\alpha(q)] < 0$. The rand-size relationship of $\alpha(0)$ was same as $D(0)$. The best-fitting model for $D(0)$, $D(1)$, $D(2)$ and $\Delta f[\alpha(q)]$ was spherical model, for $\Delta\alpha(q)$ was gaussian model, and for $\alpha(0)$ was exponential model with structure variance ratio was 1.03% , 49.83%, 0.84%, 1.48%, 22.20% and 10.60%, respectively. The results showed that soil particles of each land use pattern were distributed unevenly. The multifractal parameters under different land use have significant differences, except for $\Delta\alpha(q)$. Differences in the composition of soil particles lead to differences in the multifractal properties even though they belong to the same soil texture. Farming behavior may refine particles and enhance the heterogeneity of soil particle distribution. Our results provide an effective reference for quantifying the impact of human activities on soil system in the Three Gorges Reservoir region.

1 Introduction

Particle size distribution (PSD) is one of the essential properties used to characterize soil, which has obvious influence on the physical properties of soil such as hydraulic characteristics, soil fertility and soil erosion (Giménez et al. 1997; Huang and Zhang 2005; Montero 2005). Some natural phenomena and ecological processes could be affected by land use. Revealing the characteristics of soil PSD variation is an important part in the study of land use and management activities. In the areas with serious water and soil loss, fine particulates along with nutrients in the soil are liable to be eroded by water, and the blocking effect of different land use types on soil erosion is different (Martínez-Casasnovas and Sánchez-Bosch 2000; Basic et al. 2004). In this sense, the characteristics of soil PSD can reflect the impact of land use on erosion. What's more, some studies have linked the multifractal characteristics with soil nutrient

content to try to reveal the relationship between the multifractal characteristics and soil fertility and soil quality. For example, Sun et al. (2016) published a result that $D(1)$ and $D(2)$ were strongly positively correlated with soil organic carbon(SOC) and total nitrogen(TN) contents in the surface layers on the Loess Plateau of China. Soil PSD is still of great importance to soil water movement and soil solute migration. Hu et al. (2011) conducted an experiment about the soil PSD properties and their relationship with soil moisture and soil salinity in the mulched drip irrigated cotton fields in Xinjiang of China, suggesting that the mulched drip irrigation had a significant impact on the distribution of the soil salt.

The characteristics of PSD described as the combination of clay, silt and sand, is usually known as the texture class. A textural analysis is widely considered to be helpful in making decisions about soil conservation, productivity, and soil health. Soil samples with quite different proportions of clay, silt, and sand content might belong to a same soil texture (Filgueira et al. 2006). However, particle fractions (clay, silt, sand) do not provide enough information on soil PSD.

A detailed analysis of PSD is required to characterize soil properties. Soil PSD displays a fractal behavior (Tyler and Wheatcraft 1992; Taguas et al. 1999; Montero 2005; Prosperini and Perugini 2008; Li et al. 2011). Various studies revealed that soil texture can be described effectively by the fractal theory and analysis (Bartoli et al. 1991; Filgueira et al. 2006). Therefore, the fractal geometry was employed to explore the PSD of soil. Different fractal dimensions are obtained by using different fractal models. Generally, single fractal dimension and multiple fractal dimensions are widely used to describe soil PSD (Taguas et al. 1999; Montero 2005; De et al. 2008; Peng et al. 2014; Zhou et al. 2016; Qi et al. 2018; Wang et al. 2018). For example, Xu et al. (2013) studied the fractal characteristics of soil particle distribution and its relationship with soil TN distribution in the middle Dan River source area. Rodríguez-Lado and Lado (2017) analyzed the relationship between soil formation factors and PSD in the topsoil of Galicia by multifractal method. Single fractal can only depict characteristics of PSD in a holistic and average way, and might not always be able to evaluate the internal geometric differences, while multiple fractal theory could capture the intrinsic variability of the measure, and describe the

local heterogeneity and non-uniformity of soil PSD (Posadas et al. 2001; Paz-Ferreiro et al. 2010). Multifractal analysis distinguishes the entire volume or mass distribution of nonuniform density and represents it as a multifractal spectrum with typical shapes. Thus, in the case of soil texture, the single fractal analysis ignores the non-uniform behavior of PSD, while the multifractal analysis could take account of the changes of particle-size density, that is, the fact that some components are more frequent than others (Paz-Ferreiro et al. 2010). Thus, the multifractal technique is superior as an alternative to single fractal dimension (Grout et al. 1998).

Normally, geostatistics with a precise evaluation of spatial variation by considering the self-correlation and random variation components, is considered as an effective tool to quantify the spatial variation of various natural phenomena (Oliver 1987; Long et al. 2014). Hence, it is highly applied in spatial variation of soil properties (Trangmar et al. 1986; Cambardella et al. 1994; Tripathi et al. 2015), especially in soil PSD (Rosemary et al. 2017). Most of these studies only show the spatial distribution of single clay, silt or sand content, and cannot quantify the overall spatial variability of soil PSD. Consequently, the combination of geostatistics and multifractal is an anticipating approach to describe the subtle differences and variation trends comprehensively (Wang et al. 2018; Wang et al. 2019).

In recent years, many scholars have studied the effects of different soil types (Posadas et al. 2001; Martı et al. 2002; Montero 2005; Wang et al. 2019), land use patterns (Rodríguez-Lado and Lado 2017; Qi et al. 2018) and land restoration (Miranda et al. 2006) on the fractal characteristics of soil, to explore the relationship between fractal properties and soil characteristics. However, there are few studies on the multifractal properties of different land use patterns in purple soil areas, especially in the Three Gorges Reservoir area. Furthermore, it is essential to realize the basic spatial features of soil PSD for analyzing the spatial variation characteristics of soil nutrients, managing soil fertility, preventing and controlling soil erosion, and monitoring water quality in reservoir areas. Based on the methods of laser diffraction measurement, multifractal theory and geostatistical analysis, this study ascertained the multifractal features of the topsoil PSD, and revealed the spatial distribution of the typical agricultural catchment in this region.

2 Materials and Methods

2.1 Study area

The study area is located in the middle reaches of the Three Gorges Reservoir area (Fig. 1), named Shipanqiu in Zhong County, Chongqing municipality of China (107°3'~108°14'E, 30°03'~30°35'N). The bedrock is highly made of Jurassic Shaximiao Formation (J2s) sandstone, siltstone, and mudstone. The climate of the central region of the Three Gorge Reservoir area is a subtropical southeast monsoon with distinct seasons, abundant rainfall and sufficient sunshine. The annual average temperature of the study area is 19.2℃ with frost-free period of 320 days while the annual average rainfall is 1150 mm. However, the precipitation distributions vary unevenly with the seasons, where 70% fall in the rainy season (from April to September). The neutral purple soil is formed by a rapid weathering of sandstone siltstone and mudstone of Shaximiao Formation. The most common land use of the area includes residential areas (villages and market towns), agricultural land (dry land and paddy), orchards, forest, etc. The main crops are rice corn, potatoes, citrus, vegetables and so on.

2.2 Soil sampling

This study focused on the multifractal characteristics of topsoil at different land use patterns. In addition, 0-2 cm is the main layer of soil erosion. Therefore, the samples were collected on the topsoil (0-2 cm) of each land-use pattern. 32 samples were collected from dry land, 25 samples from paddy, 15 samples from the orchard and 12 samples from forest land, respectively. The terrain of the study area is fragmented, therefore, the number of samples depended on the area of land use and the actual distribution. Each soil sample is a mixed sample collected from multiple points (n=10) with a stainless-steel shovel to increase the representativeness of the sample, and the samples basically covered the whole catchment. However, the hydro-fluctuation belt in the south of the catchment is not included in the sampling range because it is affected by the periodic fluctuation of water level in the reservoir area. The sampling points followed the principle of random sampling. Refer to Fig. 1 for the distribution of sampling points.
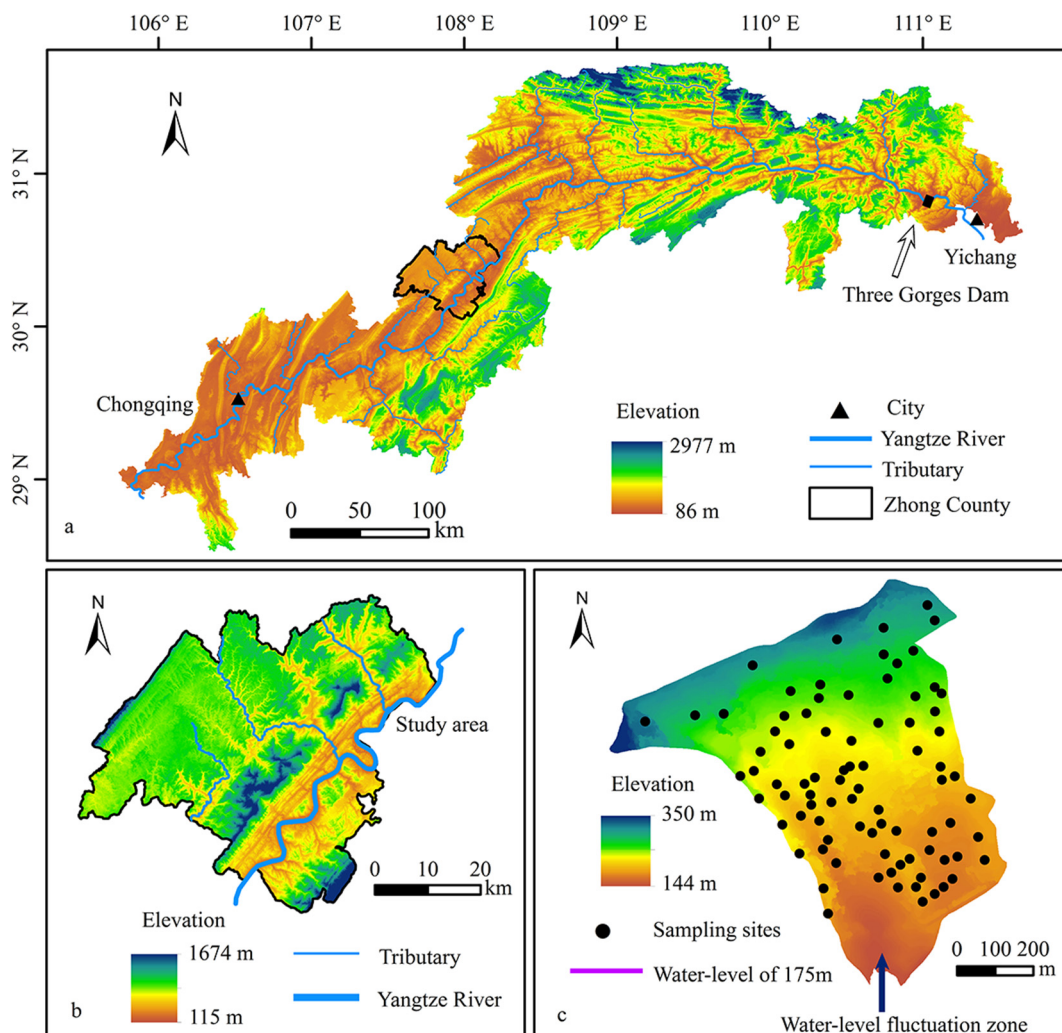
Fig. 1 (a) Elevation map of the Three Gorges Reservoir Region revealing Zhong County. (b) Elevation map of Zhong County showing Shipanqiu catchment, the study area. (c) Distribution of sampling sites in the study area.

2.3 Laboratory analyses

All samples were air-dried in the laboratory at room temperature followed by manual removal of dead leaves, plant roots, and coarse gravel. Further handling of samples involved sifting through a 2 mm soil sieve and then placing them in a labeled zip-top bag at room temperature. Soil grain size distribution was analyzed by a laser granulometer known as Malvern Mastersizer 2000 (Malvern Instruments, Malvern, England). The pre-treatment was done by adding 10% hydrogen peroxide (H_2O_2) and 10% hydrochloric acid (HCl) to remove organic matter. In addition, 10 mL Calgon (($NaPO_3$)$_6$) with a concentration of 0.05 mol L^{-1} was added and then stirred to fully separate the primary soil particles. Before laser diffraction analysis, ultrasonic dispersion for one minute was applied to samples.

2.4 Multifractal analysis of soil grain size distribution

The application principle of multi-fractal analysis in soil PSD is as follows:

The first step of the method is to subdivision of the interval. Based on the successive partitions of the interval I in dyadic scaling down and the given diameter L, dyadic partitions in k stages (k=1, 2, 3,…) generate a number $N(\varepsilon)=2^k$ of cells with equal size of $\varepsilon = L \times 2^{-k}$ to cover the entire interval I (Kravchenko et al. 1999). In present study, the first cell range of PSD is $I_1=$ [0.02, 0.024], and the last cell is $I_{64}=$ [1670.725, 2000]. As a result, the interval I = [0.02, 2000] (μm) measured by the laser particle size analyzer was divided into 64 cell intervals $I_i=$ [Φ_i, Φ_{i+1}], i=1, 2, …, 64, with the log(Φ_i/Φ_{i+1}) as a constant. After a logarithmic transformation of φ_l=log (φ_l/φ_1), for l=1,

2, ..., 65, a new dimensionless interval is formed $L=$ [0, 5] and divided into 64 subintervals of equal size, with $L_i=[\varphi_i,\varphi_{i+1}]$, $i=$1, 2, ..., 64. A number $N(\varepsilon)=2^k$ of cells is equal to size $\varepsilon=5\times2^{-k}$ for k is set up ranging from 1 to 6 (i.e., $\varepsilon=$2.5, 1.25, 0.625, 0.3125, 0.15625 and 0.078125) (Montero 2005).

Calculation of probability function is the second step. In the analysis of soil PSD, the measure p of each size sub-interval means the relative volume of soil particles at the characteristic size within the sub-interval. $p_i(\varepsilon)$ is the probability density of soil PSD within each subinterval. Construct a partition function group as follows:

$$X(q,\varepsilon) = \sum_{i=1}^{N(\varepsilon)} p_i(\varepsilon)^q \qquad (1)$$

where q is a real number.

The next step is to calculate multifractal parameters. Generalized dimensions (Rényi dimensions) are expressed as Eqs. (2) and (3) (Rényi 1955).

$$D(q) = \lim_{\varepsilon\to0} \frac{1}{q-1}\frac{\lg\left[\sum_{i=1}^{N(\varepsilon)} p_i(\varepsilon)^q\right]}{\lg\varepsilon}, \text{for } q \neq 1 \qquad (2)$$

$$D(q) = \lim_{\varepsilon\to0} \frac{\sum_{i=1}^{N(\varepsilon)} p_i(\varepsilon)\lg p_i(\varepsilon)}{\lg\varepsilon}, \text{for } q = 1 \qquad (3)$$

When $q=0$, $D(q)=D(0)$ is the capacity dimension. $D(0)$ describes the width of soil PSD. The larger $D(0)$ is, the wider distribution range of soil particle size is. Therefore, the most uneven case is $D(0)=1$, since it has the most abundant distribution of soil particles, while the most uniform distribution follows $D(0)=0$. When $q=1$, $D(q)=D(1)$ is the information dimension. $D(1)$ represents the concentration degree of PSD measure. The larger $D(1)$ is, the more discrete the soil PSD is. $D(q) = D(2)$ is the correlation dimension where $D(2)$ alone represents the symmetrical level of measuring distance of soil PSD. The larger $D(2)$ is, the more symmetrical the soil PSD is. $D(1)$ and $D(0)$ are the most frequently used multifractal parameters.

In general, the multifractal spectrum is a function of q, and the curve of the function conforms to sigmoidal shape (Montero 2005). Theoretically, q continuously varies between positive and negative infinity. However, in practice, the variation range of q is limited. In this study, the multifractal dimensions spectrum $D(q)$ was plotted within the range of $-10\leqslant q\leqslant10$ with an increment of 1 by Eqs. (2) and (3). When $D(q)$ tends to be uniformly distributed, the multifractal dimensions spectrum curve is approximate the horizontal line, which means that

PSD depicts a uniform scaling characteristics. On the other hand, When $D(q)$ conforms to the typical non-increasing s-shaped curve of theoretical multi-fractal measure, the curves have all sorts of $D(q)$ values, manifesting scaling properties of PSD varies (Montero 2005).

The multifractal singularity index $\alpha(q)$ and spectrum function $f[\alpha(q)]$ of soil PSD are computed by Eqs. (4) and (5), severally:

$$\alpha(q) = \lim_{\varepsilon\to0} \frac{\sum_{i=1}^{N(\varepsilon)} \mu_i(q,\varepsilon)\lg p_i(\varepsilon)}{\lg\varepsilon} \qquad (4)$$

$$f[\alpha(q)] = \lim_{\varepsilon\to0} \frac{\sum_{i=1}^{N(\varepsilon)} \mu_i(q,\varepsilon)\lg\mu_i(q,\varepsilon)}{\lg\varepsilon} \qquad (5)$$

where, the $\mu_i(q,\varepsilon)$ is defined as:

$$\mu_i(q,\varepsilon) = \frac{p_i(\varepsilon)^q}{\sum_{i=1}^{N(\varepsilon)} p_i(\varepsilon)^q} \qquad (6)$$

The width and symmetry of multifractal spectrum are expressed as $\Delta\alpha=\alpha(q)_{max}-\alpha(q)_{min}$ and $\Delta f(\alpha)=f[\alpha(q)_{max}]-f[\alpha(q)_{min}]$, respectively. The $\Delta\alpha$ represents the heterogeneity of soil PSD over the whole fractal structure and Δf indicates the feature of the multifractal spectrum shape and reveals the asymmetry of soil PSD. The local average singularity $\alpha(0)$ is the average singular strength of the whole multifractal structure, which is inversely proportional to the local density on the fractal structure of particle size. The greater local density of soil PSD is, the smaller $\alpha(0)$ is.

The asymmetrical $f[\alpha(q)]$ spectra is characterized as a right-skewed spectrum when $\Delta f > 0$, as a left-skewed spectrum when $\Delta f <0$ while asymmetric shape appears when $\Delta f =0$. Indeed, the more right-skewed multifractal spectrum, the more significant impact of low-value information of the variable on the soil PSD. Conversely, the high value information has a more significant impact on the soil PSD (Guan et al. 2007; Wang et al. 2018).

2.5 Geostatistical analysis of soil PSD multifractal properties

The key of geostatistics method is to explore the spatial variability of PSD multifractal parameters by using the semi-variogram, and determine the optimal input parameters for Kriging interpolation.

In this study, the semi-variogram of each multifractal parameters of soil PSD was calculated by Eq. (7):

$$\gamma(h) = \frac{1}{2N(h)}\sum_{i=1}^{N(h)}[Z(x_i) - Z(x_i + h)]^2 \qquad (7)$$

where $\gamma(h)$ is the semi-variance of the lag interval h,

reflecting the spatial relationship between adjacent sampling points. $Z(x_i)$ and $Z(x_i+h)$ are the measured variables for the positions of x_i and x_i+h, and N(h) is the number of pairs spaced by a given distance h.

The calculation of semi-variograms is subsequently followed by selecting one fitting theoretical model among Gaussian model (Eq. 8), spherical model (Eq. 9) and exponential model (Eq. 10), which are widely used in soil research.

The Gaussian semivariogram function is:

$$\gamma(h) = \begin{cases} 0, \text{for } h = 0 \\ C_0 + C\left[1 - \exp\left(-\frac{h^2}{a^2}\right)\right], \text{ for } h > 0 \end{cases} \quad (8)$$

The spherical semivariogram function is:

$$\gamma(h) = \begin{cases} C_0 + C\left[\frac{3h}{2a} - \frac{h^3}{2a^3}\right], \text{for } h \le a \\ C_0 + C, \text{ for } h \ge a \end{cases} \quad (9)$$

The exponential semivariogram function is:

$$\gamma(h) = \begin{cases} 0, \text{for } h = 0 \\ C_0 + C\left[1 - \exp\left(-\frac{h}{a}\right)\right], \quad \text{for } h > 0 \end{cases} \quad (10)$$

where C_0 is the nugget effect, C_0+C is the sill or total variance, and a is the range of spatial dependence.

Semi-variograms can analyze and explain the spatial distribution and structural characteristics of the regionalized variables, at the same time it provides relevant information for kriging spatial interpolation. Variables including the sill (C_0+C), the nugget (C_0) and the spatial structure ratio [$C_0/(C_0+C)$] were used to evaluate the spatial dependence of soil PSD multifractal parameters. As the lag distance increases, a threshold can be reached to measure spatial heterogeneity, if the variogram stabilizes. The distance at which the variogram reaches the sill is called the range (a). Nugget is defined as the variability at a scale smaller than the sampling interval and the error of sampling analytical. Spatial structure ratio which is the ratio of nugget to sill value reflects the degree of spatial auto-correlation. When the value of [$C_0/(C_0+C)$] is ≤25%, it is deemed to be strongly spatial autocorrelation. When [$C_0/(C_0+C)$] is between 25% and 75%, it is assumed to be moderately spatial autocorrelation. Further increase of this ratio

to where [$C_0/(C_0+C)$]>75%, it is considered as a weakly spatial autocorrelation (Cambardella et al. 1994; Wang et al. 2018).

The Kriging interpolation method, also known as spatial topo-interpolation method is based on spatial correlation, variogram theory and structural analysis. It plays a major role in geostatistics research, primarily for unbiased optimal estimation of variables in a limited region. Generally, Kriging estimates can be calculated by Eq. (11):

$$Z(x_0) = \sum_{i=1}^{n} \lambda_i Z(x_i) \quad (11)$$

where $Z(x_0)$ is the estimated value of sampling site x_0; $Z(x_i)$ is a given value at location of x_i; and λ_i is weight coefficient. The magnitude of n depends on the size of the moving search window and user definition.

The geostatistical analysis was performed by GS+9.0. The general trend of the data can be revealed by the Kriging estimates map accomplished by software ArcGIS 10.3 (Esri, Redlands, California, USA).

3 Results

3.1 Soil particle fractions of different land use patterns

The soil particle fractions (clay, silt, sand) of different land use patterns in the study area were presented in Table 1. Median particle size (d_{50}) is an important index of soil particle distribution. Normally, the median particle size varies according to different land use patterns. The maximum median particle size for forest land is 52.55μm, which is significantly larger than dry land, orchard and paddy. The smallest median particle size was found in paddy with 28.62 μm which is highly different from other land use patterns, though orchard exhibited the exception. In addition, its clay content was also significantly higher than other studied land use patterns. Generally, silt accounted for the largest proportions in the composition of soil particles for all land use patterns with the values ranging from 49.30% to 59.42%, sand

Table 1 Soil particle fractions of four land use patterns in Shipanqiu catchment, Chongqing municipality of China

Land use patterns	Vegetation types	Median particle size d_{50} (μm)	Clay (%) (<0.002mm)	Silt (%) (0.002-0.05 mm)	Sand (%) (0.05-2 mm)
Dry land	Annual herbs (rape, corn, potato)	37.19±18.69 B	2.04±0.83B	57.38±10.66 A	40.58±11.23B
Forest	Perennial trees (bamboo)	52.55±23.52A	1.91±0.61B	49.30±8.68 B	48.79±8.98 A
Orchard	Small perennial trees (citrus)	33.39±9.75 BC	1.67±0.52 B	58.27±6.66 A	40.06±6.94 B
Paddy	Annual grass (paddy)	28.62±8.68 C	3.16±0.99A	59.42±6.41 A	37.41±6.96 B

Note: Value in table is mean ± standard deviation. Different uppercase letters in one same column mean significant difference ($P<0.05$)

grains were slightly less than silt content with the proportions ranging from 37.41% to 48.79%, while the percent of clay particles were tiny less than 5%, respectively. According to the USDA soil texture classification standard, the soil of four land use patterns in this study were silty loam and sandy loam (Fig. 2).

3.2 Multifractal characteristics

The multifractal analysis can be carried out when the logarithmic curves of the partition function $X(q, \varepsilon)$ and the box scale (ε) satisfy a linear relationship. Fig. 3 showed the log-log curves (for $-10 \leqslant q \leqslant 10$) of the partition function $X(q, \varepsilon)$ and box scale (ε) of a random soil sample, with coefficient of determination between 0.93 and 0.99 (Table 2). It indicated that the soil samples in the study area have multifractal characteristics.

According to the multi-fractal algorithm, the soil particle sizes of different land use patterns in the study area were analyzed. Within the range of $-10 \leqslant q \leqslant 10$, the generalized dimension spectrum $D(q)$ of PSD was obtained, as illustrated in Fig. 4. The trend of generalized dimension spectrums of the four land use patterns was basically consistent ranging from 0.8 to 2.0. Indeed, they showed a distinct variation across negative values of q. When $q>0$, $D(q)$ highlights the property of large probability measure range, which can reflect the overall complexity of PSD. Contrary, when $q<0$, $D(q)$ represents the property of small probability measure interval, and this reflects the small and complex features of PSD fractal structure. In general, when $q<0$, the variation range of $D(q)$ is greater than $q>0$, which indicates that soil particles distributed in dense areas of these 4 land use patterns have better scaling than those in sparse areas. That is, $D(q)$ is more accurate in the region of small probability measure than in the region of large probability measure. For all land use studied, orchard showed the largest monotonic decline, while forest revealed the smallest
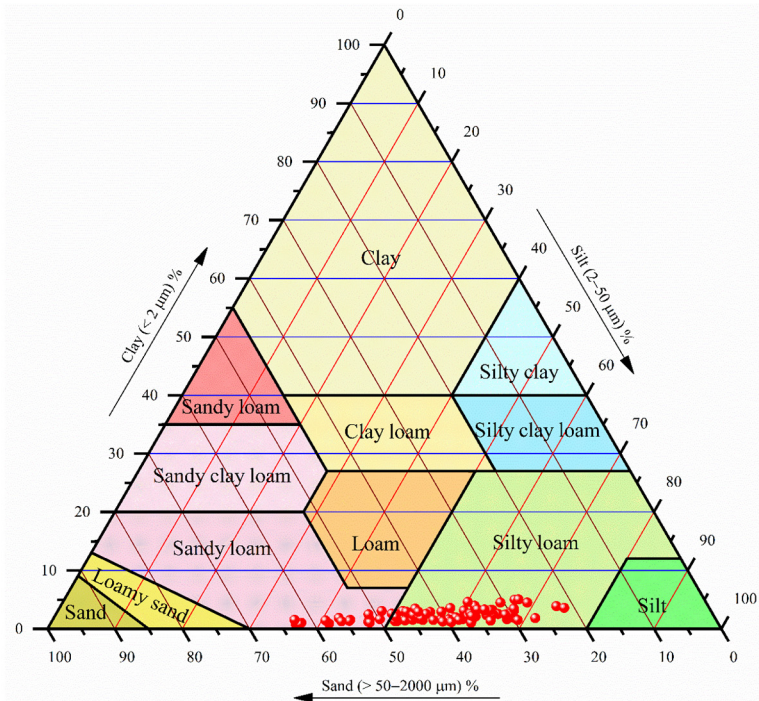

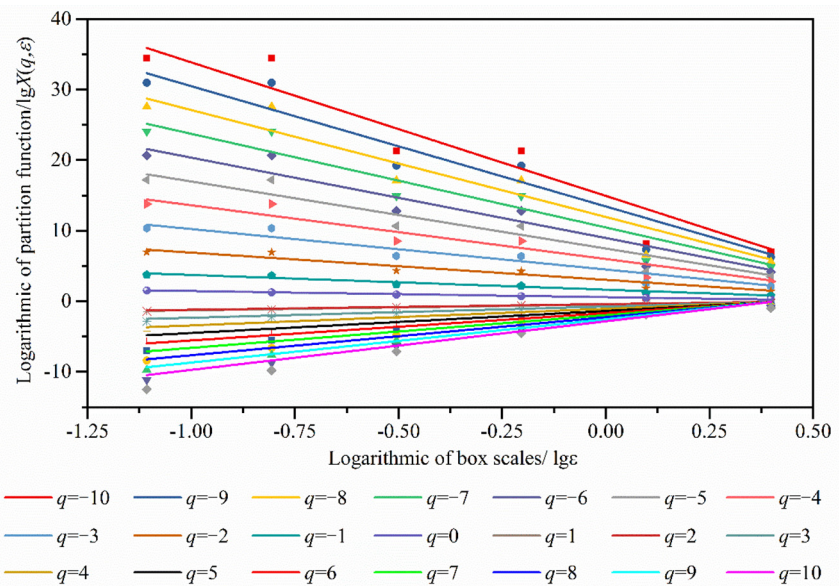**Fig. 2** Soil texture classification of Shipanqiu catchment.

Fig. 3 Log-log plots of partition functions $X(q, \varepsilon)$ and measurement scales (ε) of soil particle size distribution.

decrease. It signified that the PSD of orchard had a stronger nonuniformity, while forest presented more evenly.

The statistical information of six multifractal parameters, which included capacity dimensio n $D(0)$, information dimension $D(1)$, the correlation dimension $D(2)$, the multifractal spectrum width $\Delta\alpha(q)$, the multifractal spectrum symmetry $\Delta f[\alpha(q)]$, and the local average singularity $\alpha(0)$ for different land-use patterns are presented in Fig. 5. The median values of the vast majority of multifractal attributes are approximate their mean value, and the median values are less sensitive than the mean when the number of samples studied is relatively small, therefore, the median values were selected for further analyses.

The capacity dimension ($D(0)$) of the four land use patterns are ranked as: dry land < orchard < forest < paddy. It implies that the width of soil PSD in paddy is the widest, which may due to the smallest grain size of the soil in the paddy. Contrary, dry land has the narrowest scope of soil PSD. The variation range of ($D(0)$) were 0.803~0.870, 0.838~0.872, 0.838~0.923, 0.816~0.888, respectively, corresponding to dry land, orchard, paddy, forest. Our results for the information dimension ($D(1)$) showed that dry land has the lowest value, while forest land has the highest value. It demonstrated that the PSD of forest is more discrete than other three kinds of land use patterns whereas the PSD for dry land is highly concentrated.
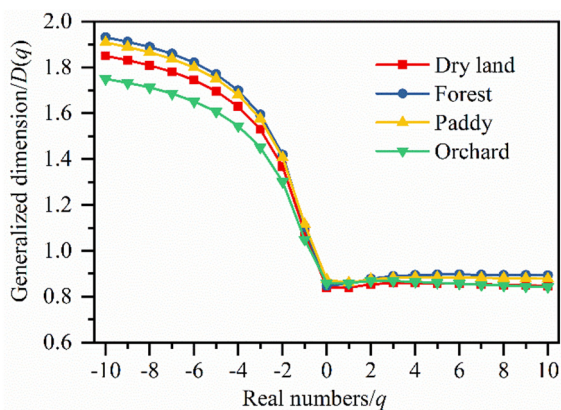
Table 2 Log–log fitting of the partition function [lg $X(q,\varepsilon)$] and box scale (lgε) of a random soil sample in the interval $-10 \leqslant q \leqslant 10$.

Equation	Plot	Intercept	Slope	r	R-square (COD)
$y = a + bx$	$q=-10$	14.94	-18.93	-0.96	0.93
	$q=-9$	13.44	-17.05	-0.96	0.93
	$q=-8$	11.95	-15.16	-0.96	0.93
	$q=-7$	10.46	-13.27	-0.96	0.93
	$q=-6$	8.97	-11.39	-0.97	0.93
	$q=-5$	7.48	-9.50	-0.97	0.93
	$q=-4$	5.99	-7.62	-0.97	0.94
	$q=-3$	4.51	-5.73	-0.97	0.94
	$q=-2$	3.04	-3.86	-0.97	0.95
	$q=-1$	1.65	-2.09	-0.99	0.97
	$q=0$	0.58	-0.86	-1.00	0.99
	$q=1$	-0.46	0.82	0.98	0.97
	$q=2$	-0.40	0.80	0.98	0.96
	$q=3$	-0.75	1.58	0.98	0.96
	$q=4$	-1.06	2.36	0.98	0.96
	$q=5$	-1.37	3.12	0.98	0.96
	$q=6$	-1.67	3.88	0.98	0.96
	$q=7$	-1.96	4.64	0.98	0.95
	$q=8$	-2.25	5.39	0.98	0.95
	$q=9$	-2.54	6.14	0.98	0.95
	$q=10$	-2.83	6.89	0.98	0.95

Note: r =Pearson correlation coefficient; COD=Coefficient of determination.

Furthermore, the PSD of orchard and paddy showed a similar dispersion. The value range of ($D(1)$) of dry land, orchard, paddy, and forest were 0.816~0.860, 0.839~0.872, 0.842~0.926, 0.834~0.878, severally. The correlation dimension ($D(2)$) presented a rand-size relationship as dry land < forest < paddy < orchard. As a result, the results for this parameter indicated that the PSD of orchard is the most symmetrical, followed by paddy and forest, finally dry land found to be the least symmetrical land use. Therefore, it is asymmetrical for the PSD in four kinds of land use patterns.

Different from the generalized dimension spectrum, multifractal singular spectrum function characterizes part features of fractal structure. In this study, the multifractal spectrum curve drawn according to $\alpha(q)$ and $f[\alpha(q)]$ was a unimodal function with a high coincidence degree and a left-skewed shape (Fig. 6). It indicated that coarse particles of purple soil dominated the distribution of soil size, and the degree of variability was greater than that of fine particles. The left branch of the multifractal singular spectral function of PSD in the four land use patterns was similar, while the right branch showed some differences in the width and the symmetry of spectrum. The spectral width $\Delta\alpha(q)$ may be related to
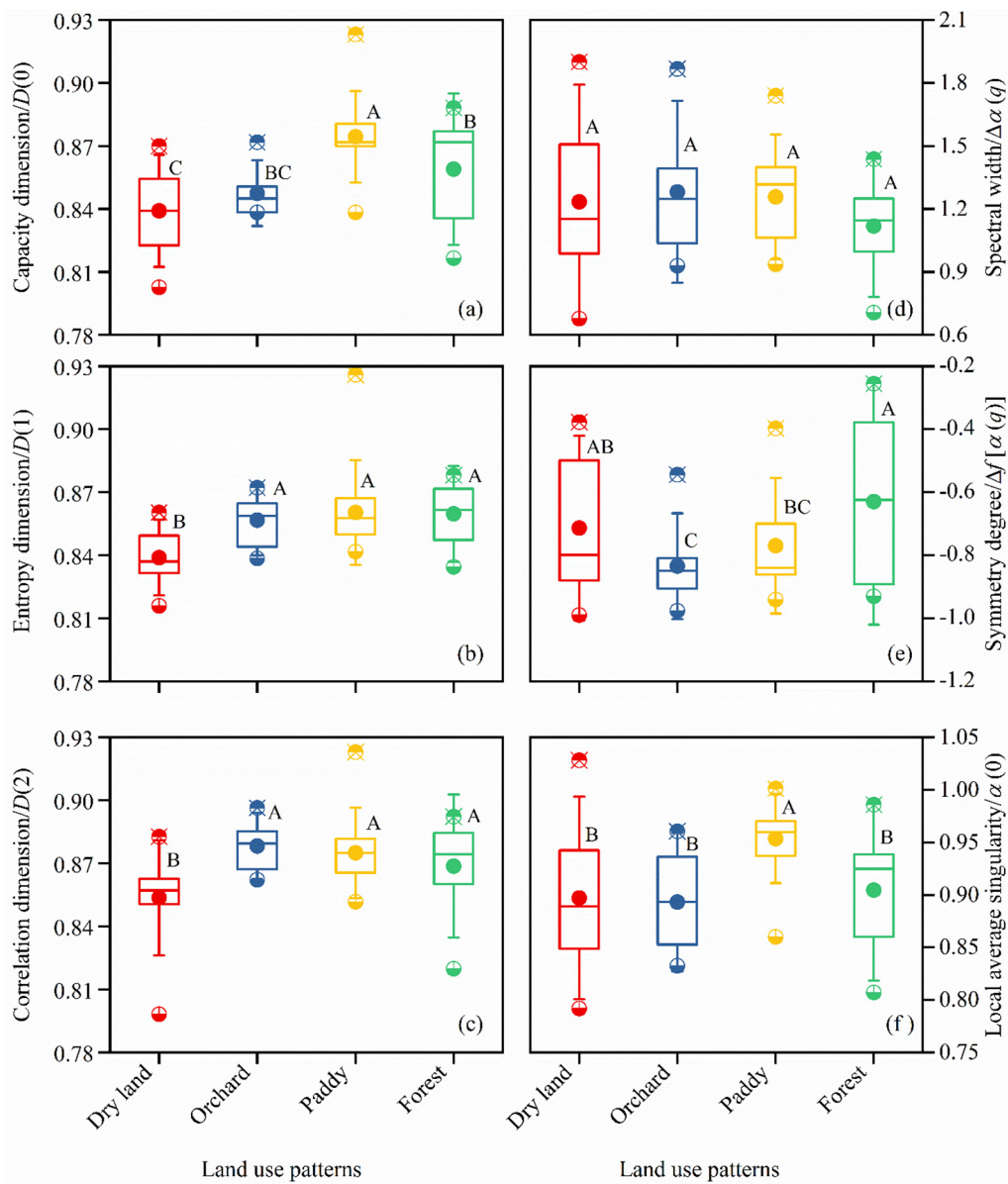

Fig. 4 Generalized dimension spectrums of particle size distribution in different land use patterns of Shipanqiu catchment.

Fig. 5 Statistics of six multifractal parameters in four kinds of land-use patterns of Shipanqiu catchment. The boxplot with different letters in each multifractal parameter indicates significant difference at *P*<0.05. The upper and lower points outside the boxplot represent the maximum and minimum values, the points inside the boxplot represent the average value, and the box from up to down represent the upper quartile, median and lower quartile respectively.

the heterogeneity (Paz-Ferreiro et al. 2010; San José Martínez et al. 2010). However, the $\Delta\alpha(q)$ values of dry land, orchard, and paddy were quite similar, which concentrated between 1.0 and 1.3, indicating a similar degree of heterogeneity for the four kinds of land use patterns studied. In addition, $\Delta f[\alpha(q)]<0$ in all land use patterns revealed that larger volume fraction of particles in the dominant position (Paz-Ferreiro et al. 2010; San José Martínez et al. 2010). The rand-size relationship of local average singularity ($\alpha(0)$) was in the order as: dry land<

orchard<forest<paddy. The local density of soil particles in dry land was the highest, followed by orchards and forest, and paddy field was the smallest.

Some parameters were found to be correlated (Table 3). Parameter pairs with significant positive correlation coefficients were $D(0)$ and $D(1)$ (0.669), $D(0)$ and $D(2)$(0.470), $D(0)$ and $\Delta\alpha(q)$ (0.289), $D(0)$ and $\alpha(0)$ (0.777), $D(1)$ and $D(2)$ (0.819), $\Delta\alpha(q)$ and $\alpha(0)$ (0.624), while the significant negative correlations appeared in $D(2)$ and $\Delta f[\alpha(q)]$ (-0.372), $\Delta\alpha(q)$ and $\Delta f[\alpha(q)]$ (-0.344), $\Delta f[\alpha(q)]$ and $\alpha(0)$ (-0.248).

3.3 Relationship between multifractal parameters and soil particle composition

According to the Pearson correlation analysis of multiple fractal parameters and soil texture (Table 3), soil texture and multifractal parameters were in varying degrees of correlation. There was a positive correlation between clay and $D(0)$(0.604), clay and $\Delta\alpha(q)$(0.314), clay and $\alpha(0)$(0.742), silt and $\Delta\alpha(q)$(0.352), silt and $\alpha(0)$ (0.435), sand and $D(1)$(0.251), sand and $\Delta f[\alpha(q)]$ (0.706). Moreover, a significantly negative correlation between clay and $\Delta f[\alpha(q)]$ (-0.350), silt and $D(1)$(-0.270), silt and $\Delta f[\alpha(q)]$ (-0.710), sand and $\Delta\alpha(q)$(-0.365), sand and $\alpha(0)$ (-0.487) was found.

3.4 Geostatistical analysis

The best-fitting semi-variogram model and related parameters of multifractal attributes were listed in Table 4. No conversion was conducted to the data since no significant trends were found. The structure variance ratio ($[C_0/(C_0+C)]$) was used to estimate the spatial variation degree of parameters. The spherical model calculated by semi-variogram was applicable to the parameters $D(0)$, $D(1)$, $D(2)$, and $\Delta f[\alpha(q)]$ $[C_0/(C_0+C)]$ ratios were 1.03% , 49.83%, 0.84%, and 1.48%, respectively. A gaussian model was detected as the appropriate for $\Delta\alpha(q)$ with a value of 22.20% for $[C_0/(C_0+C)]$. However, the optimal fitting model for $\alpha(0)$ was the exponential model, with a structure variance ratio of 10.60%. It was apparent that the parameters $D(0)$, $D(2)$, $\Delta\alpha(q)$, $\Delta f[\alpha(q)]$ and $\alpha(0)$ showed a relatively weak spatial variability in the experimental site because of their structural variance ratio below 25%. Parameter $D(1)$ performed moderate variation, since its structural variance ratio is between 25% and 75%. It could be noticed that no parameters presented a strong spatial variation in the studied catchment.

The result of spatial variability is a prerequisite for drawing kriging graphs of different multifractal parameters in PSD. Based on the semi-variogram model, the multi-fractal parameters of soil PSD were visualized by mapping the spatial distribution of $D(0)$, $D(1)$,$D(2)$, $\Delta\alpha(q)$, $\Delta f[\alpha(q)]$ and $\alpha(0)$ by means of ordinary kriging interpolation. The results of interpolation for each parameter are displayed in Fig. 7. Maps of multifractal parameters were drawn at the same scale to facilitate comparative analysis.
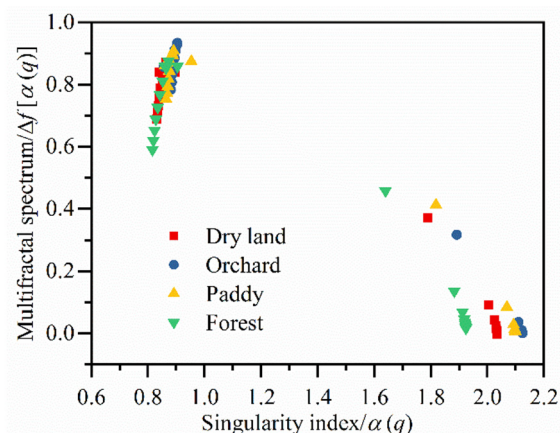
The spatial distribution trend varied with

Fig. 6 Multifractal spectra of soil particle size distribution for different land-use patterns of Shipanqiu catchment.

multifractal parameters. $D(0)$ (Fig. 7 (a))has two hot spots. One neared the southwest boundary, and the other approached in the southeast of the study area. With these two hot spots as the center, the value of $D(0)$ decreased in all directions, and the minimum value was mainly concentrated in the northeast corner. This result may be affected mostly by the pattern of land use. The large region of the southwest boundary was occupied by forest, the northeastern primarily occupied by orchard, and the southeastern was mainly filled with paddy and dry land. The terrain of the experimental area is broken, paddy fields and dry lands crisscross.

The low value of $D(1)$ (Fig. 7(b)) appeared along the northwest to southeast of the research area and then increased on both sides, and the high values were reached in the northwest corner, along the southwest and eastern (except the northeast and southeast corners) of the study area, respectively. The high, middle and low value areas were clearly demarcated and presented obvious banding distribution. The distribution of $D(2)$ (Fig. 7(c)) had obvious regional characteristics. Based on the distribution, study area was divided into three sections, in which the northwestern and southeastern were low-value areas, and the large area which including the western, northeastern and eastern areas was high-value area. Moreover, as for $\Delta\alpha(q)$ (Fig. 7(d)), the relative high-value regions distributed in the central part and southeast corner of the catchment, while the relative low-value regions concentrated along western boundary and northwest corner. The distribution of $\Delta f[\alpha(q)]$ (Fig. 7(e)) has a hot spot located in the northwestern, and an evident

low-value area appeared in the northeast corner of the catchment. In addition, parameter $\alpha(o)$ (Fig. 7(f)) showed that the high values were concentrated in southeastern regions, while the low values distributed in northeastern.

4 Discussion

4.1 PSD characteristics

In terms of the percentage of soil PSD, the silt content (49.30%~59.42%) was dominant under different land use patterns in the study area, followed by sand grains (37.41%~48.79%), with the clay content (1.67%~3.16%) being the lowest. Compared with forest, the other three patterns of land use significantly reduced the contents of sand, and significantly increased silt content. The effect of land use on clay content was not statistically significant except for paddy (Table 1). It indicated that the distribution of soil particles in the study area was concentrated and non-uniform. As a result, it is necessary to conduct multifractal analysis. Purple soil is a kind of soil developed from sedimentary rocks,

which has marked soil coarseness, with an evident soil erosion characteristic. The median particle size (d_{50}) of four land-use patterns presented a relationship as: forest > dry land > orchard > paddy. The soil studied was disturbed by human activities for a long time except forest. To some extent, this demonstrated that long-term tillage had a refining effect on coarse soil particles. The composition of soil particles is also related to the type of vegetation, besides the soil parent material and physiochemical weathering (Qi et al. 2018). The growth of plant roots and the decomposition of litter would affect the physicochemical and biological properties of soil, and then affect the composition of soil particles. Annual herbs are main crops of dry land, such as canola, corn, potato, and so on, with sparse, fine root systems and little surface litter. However, the citrus orchard is a mature dungarunga with complex root network and affluent surface litter. The cementing substances secreted by the root effectively facilitate the formation of soil aggregates to improve soil fertility, enhance soil stability, improve the physical and chemical properties of soil, and thus promote the increase of fine particulate and the decrease of coarse particle content (Posadas et al. 2001; Su et al. 2018).

Table 3 Pearson correlation analysis of soil texture and multiple fractal parameters

Multifractal parameters	Clay	Silt	Sand	Capacity dimension $D(o)$	Entropy dimension $D(1)$	Correlation dimension $D(2)$	Spectral width $\Delta\alpha(q)$	Symmetry degree $\Delta f[\alpha(q)]$	Local average singularity $\alpha(o)$
Clay	1								
Silt	0.512**	1							
Sand	-0.586**	-0.996**	1						
Capacity dimension $D(o)$	0.604**	0.042	-0.101	1					
Entropy dimension $D(1)$	0.037	-0.270*	0.251*	0.669**	1				
Correlation dimension $D(2)$	0.114	0.183	-0.184	0.470**	0.819**	1			
Spectral width $\Delta\alpha(q)$	0.314**	0.352**	-0.365**	0.289**	-0.049	0.066	1		
Symmetry degree $\Delta f[\alpha(q)]$	-0.350**	-0.710**	0.706**	0.015	0.101	-0.372**	-0.344**	1	
Local average singularity $\alpha(o)$	0.742**	0.435**	-0.487**	0.777**	0.131	0.158	0.624**	-0.248*	1

Note: ** and * are significant at conference levels of 0.01 and 0.05, respectively.

Table 4 Fitting semivariogram models for multifractal parameters of soil particle-size distribution

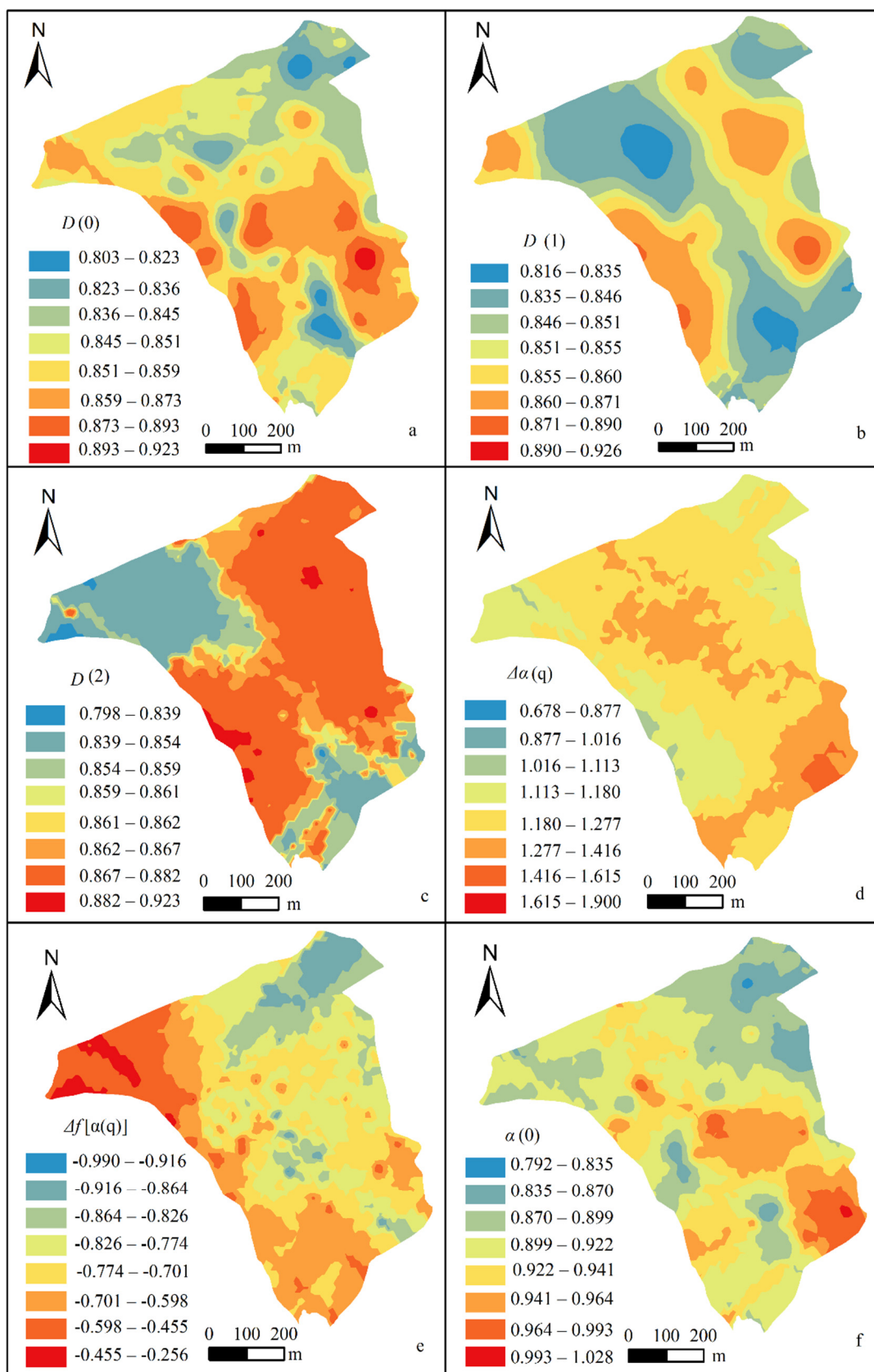| Multifractal parameters	Fitting model	Nugget (C_0)	Sill (C_0+C)	Structure variance ratio [$C_0/(C_0+C)$, %]
$D(o)$	Spherical	0.000005	0.000486	1.03
$D(1)$	Spherical	0.000149	0.000299	49.83
$D(2)$	Spherical	0.000003	0.000359	0.84
$\Delta\alpha(q)$	Gaussian	0.093000	0.418853	22.20
$\Delta f[\alpha(q)]$	Spherical	0.000500	0.033700	1.48
$\alpha(o)$	Exponential	0.000339	0.003198	10.60

Fig. 7 Spatial distribution of multifractal parameters of soil particle size distribution in Shipanqiu catchment.

4.2 Multifractal parameters

The multifractal method applied in soil could capture more detailed information on soil PSD and reflect the change of soil physical characteristics (Xu et al. 2013). The generalized dimension ($D(q)$, as shown in Fig. 4) quantifies the statistical properties of the fractal measure and quantifies the complexity and non-uniformity of the soil PSD fractal structure at different levels. The values of generalized dimension spectrums of the four land-use patterns ranged from 0.8 to 2.0. A similar outcome had been presented in Qi et al. (2018), ranging from 0.8 to 2.3 for Oak forest land, within the scope of 0.7 to 1.9 for terraced farmland, 0.7~1.8 for shrub-grass sloping land and sloping farmland. Xia et al. (2020) calculated the generalized dimension spectrums of four different vegetation types: shrub-grass community of *Ziziphus jujuba var. spinosa-Artemisia mongolica* (0.5~2.3), shrub-grass community of *Periploca sepium Bunge-Messerschmidia sibirica* (0.5~1.6), mixed herbaceous community of *Artemisia mongolica-Phragmites australis* (0.5~1.5), and bare land (0.5~1.0). The generalized dimensional spectrum of soils disturbed by human activities over time may vary more widely than that of soils hardly disturbed, such as woodlands and shrub lands. Tillage behavior probably enhanced the heterogeneity of soil particle distribution.

Capacity dimension $D(0)$ represents the width range of soil PSD. The larger the $D(0)$ is, the wider the soil PSD. The range of $D(0)$ under four kinds of land use in the research area was 0.803~0.923. Similar results have been reported by Martı et al. (2002), indicating that the value of ($D(0)$) varied from 0.83 to 1.0 of twenty mineral soils. Paz-Ferreiro et al. (2010) presented the results ranging from 0.923 to 1.0 for 32 study PSDs under two tillage treatments and two cropping systems. Rodríguez-Lado and Lado (2017) found a range of 0.831~0.975 for ($D(0)$). Moreover, Montero (2005) published a narrow range of 0.95~0.99 of ($D(0)$). Information dimension $D(1)$ measures the concentration of soil PSD, which is connected with the degree of soil evolution (Martı et al. 2002; Rodríguez-Lado and Lado 2017). Various studies found different ranges of the information dimension. Montero (2005) found a variation range of ($D(1)$) between 0.77~0.88, Paz-Ferreiro et al. (2010) introduced a range of 0.859~0.921, and Martı et al. (2002) reported a range of 0.75~0.95, Rodríguez-Lado and Lado (2017) published a range of

0.772~0.934. The larger correlation dimension $D(2)$ is, the more uniform the PSD is, in the measurement interval. The relationship between $f[\alpha(q)]$ and $\alpha(q)$ could provide more information of fractal structure.

Different land use patterns have a great influence on soil particle evolution. The multifractal parameters are closely related to the composition of soil particles. As for the parameters in the generalized dimension, a significant positive correlation was found between $D(0)$ and clay content. A similar result was shown in Qi et al. (2018). The value variation range of clay content of collected samples was small, correspondingly, the difference of $D(0)$ under different land use patterns was not obvious. Parameter $D(1)$ presented a positive correlation with sand content, and a negative correlation with silt content. However, some existing studies have represented a significant relationship between $D(1)$ and clay particles (Miranda et al. 2006; De et al. 2008). No significant relationship between $D(2)$ and soil particle volume fraction was demonstrated in this study. However, previous studies have shown some other results. Negative correlations were found between $D(2)$ and clay content in the study of Miranda et al. (2006), while positive correlations were exhibited between $D(2)$ and clay content in Qi et al. (2018). $\Delta\alpha(q)$ and $\alpha(0)$ were positively related with clay and silt content, negatively related with sand content while $\Delta f[\alpha(q)]$ was positively related with sand content and negatively related with clay and silt content. The above-mentioned results are slightly different from previous studies. The findings of Sun et al. (2016) reported that $D(1)$ and $D(2)$ were positively correlated with clay and silt content, negatively correlated with sand content while $\Delta\alpha(q)$ was positively correlated with clay content and negatively correlated with sand content. Consequently, the soil particle composition (clay, silt, sand content) had a great influence on symmetry, heterogeneity, and average singular strength of the whole multifractal structure. Posadas et al. (2001) found that the proportional allocation of clay, silt and sand content affected the scale properties of single fractal and multifractal. The high probability subsets of purple soil were mainly concentrated in silt and sand grains due to their absolute dominance in soil composition. Although the volume fraction of clay was extremely small, it may have an unexpected influence on multifractal parameters. Posadas et al. (2001) arrived at a conclusion that clay particles were the most important factor affecting heterogeneity, and the heterogeneity of distribution increased with the increase of clay content.

The relationship between soil PSD and multifractal properties varies from study to study. Further research is needed to find out the reasons for the inconsistent results among different studies.

4.3 Spatial distribution characteristics

Spatial distribution characteristic of the 6 parameters in the catchment exhibited a relatively weak and moderate spatial variability, without strong variation. A small area (0.51 km²) of the catchment could be the main reason, sharing the same climate and parent material, which are major factors to affect the characteristic of soil PSD in a large scale (Rodríguez-Lado and Lado 2017). On the other hand, three kinds of land-use patterns (dry land, orchard, paddy) were subject to long-term interference from human farming activities, which also accounted for the mild spatial variation characteristic. Besides, fragmented and interlaced terrain may also be a factor.

5 Conclusions

This study explored the multifractal properties and spatial distribution characteristics of soil PSD in a representative agricultural catchment of the Three Gorges Reservoir area by methods of multifractal theory and geo-statistics. The results indicated that soil particles for different land use patterns were not evenly distributed in the study area. In addition, the coarse particles (sand and silt) were dominant in purple soil, and the degree of variation was greater than that of fine particles (clay). The changes in the dense distribution area of purple soil particles can be better reflected by the generalized dimension spectrum compared to the sparse distribution area. Eminently, forest land has a stronger even grain size distribution among the four patterns of land use studied. Tillage activities may make the distribution of soil particles more uneven. The four land-use patterns in this study have significant impacts on multifractal parameters except spectral width ($\Delta\alpha(q)$). Thus, these parameters can be used to reflect the impact of land use on soil physical properties.

Our work focused exclusively on multifractal features in different land-use patterns and the spatial variability of soil PSD. Divergent trends in the spatial variability of multi-fractal parameters of soil PSD were found in the experimental site. Accordingly, further researches should be conducted on the reasons for this difference.

Acknowledgements

References

Bartoli F, Philippy R, Doirisse M, et al. (1991) Structure and self-similarity in silty and sandy soils: the fractal approach. J Soil Sci 42: 167-185.
https://doi.org/10.1111/j.1365-2389.1991.tb00399.x

Basic F, Ivica K, Mesic M, et al. (2004) Tillage and crop management effects on soil erosion in central Croatia. Soil Till Res 78: 197-206.
https://doi.org/10.1016/j.still.2004.02.007

Cambardella CA, Moorman TB, Parkin TB, et al. (1994) Field-Scale Variability of Soil Properties in Central Iowa Soils. Soil Sci Soc Am J 58: 1501-1511.
https://doi.org/10.2136/sssaj1994.03615995005800050033x

De W, Fu B, Zhao W, et al. (2008) Multifractal characteristics of soil particle size distribution under different land-use types on the Loess Plateau, China. Catena 72: 29-36.
https://doi.org/10.1016/j.catena.2007.03.019

Filgueira RR, Fournier LL, Cerisola CI, et al. (2006) Particle-size distribution in soils: A critical study of the fractal model validation. Geoderma 134: 327-334.
https://doi.org/10.1016/j.geoderma.2006.03.008

Giménez D, Perfect E, Rawls WJ, et al. (1997) Fractal models for predicting soil hydraulic properties: A review. Eng Geol 48: 161-183.
https://doi.org/10.1016/S0013-7952(97)00038-0

Grout H, Tarquis AM, Wiesner MR (1998) Multifractal Analysis of Particle Size Distributions in Soil. Environ Sci Technol 32: 1176-1182.
https://doi.org/10.1021/es9704343

Guan X, Yang P, Ren S, et al. (2007) Multifractal analysis of soil structure under long‐term wastewater irrigation based on digital image technology. New Zeal J Agr Res 50: 789-796.
https://doi.org/10.1080/00288230709510352

Hu H, Tian F, Hu H (2011) Soil particle size distribution and its relationship with soil water and salt under mulched drip irrigation in Xinjiang of China. Sci Chin Technol Sci 54: 1568.
https://doi.org/10.1007/s11431-010-4276-x

Huang G, Zhang R (2005) Evaluation of soil water curve with the pore-solid fractal model. Geoderma 127: 52-61.
https://doi.org/10.1016/j.geoderma.2004.11.016

Kravchenko AN, Boast CW, Bullock DG (1999) Multifractal

Analysis of Soil Spatial Variability. Agron J 91: 1033-1041. https://doi.org/10.2134/agronj1999.9161033x (English)

Li Y, Li M, Horton R (2011) Single and Joint Multifractal Analysis of Soil Particle Size Distributions. Pedosphere 21: 75-83. https://doi.org/10.1016/S1002-0160(10)60081-1

Long X-H, Zhao J, Liu Z-P, et al. (2014) Applying geostatistics to determine the soil quality improvement by Jerusalem artichoke in coastal saline zone. Ecol Eng 70: 319-326. https://doi.org/10.1016/j.ecoleng.2014.06.024

Martı, x, n MÁ, et al. (2002) Laser diffraction and multifractal analysis for the characterization of dry soil volume-size distributions. Soil Till Res 64: 113-123. https://doi.org/10.1016/S0167-1987(01)00249-5

Martínez-Casasnovas JA, Sánchez-Bosch I (2000) Impact assessment of changes in land use/conservation practices on soil erosion in the Penedès–Anoia vineyard region (NE Spain). Soil Till Res 57: 101-106. https://doi.org/10.1016/S0167-1987(00)00142-2

Miranda JGV, Montero E, Alves MC, et al. (2006) Multifractal characterization of saprolite particle-size distributions after topsoil removal. Geoderma 134: 373-385. https://doi.org/10.1016/j.geoderma.2006.03.014

Montero Es (2005) Rényi dimensions analysis of soil particle-size distributions. Ecol Model 182: 305-315. https://doi.org/10.1016/j.ecolmodel.2004.04.007

Oliver MA (1987) Geostatistics and its application to soil science. Soil Use Manage 3: 8-20. https://doi.org/10.1111/j.1475-2743.1987.tb00703.x

Paz-Ferreiro J, Vázquez EV, Miranda JGV (2010) Assessing soil particle-size distribution on experimental plots with similar texture under different management systems using multifractal parameters. Geoderma 160: 47-56. https://doi.org/10.1016/j.geoderma.2010.02.002

Peng G, Xiang N, Lv S-q, et al. (2014) Fractal characterization of soil particle-size distribution under different land-use patterns in the Yellow River Delta Wetland in China. J Soils Sediments 14: 1116-1122. https://doi.org/10.1007/s11368-014-0876-6

Posadas AND, Giménez D, Bittelli M, et al. (2001) Multifractal Characterization of Soil Particle-Size Distributions. Soil Sci Soc Am J 65: 1361-1367. https://doi.org/10.2136/sssaj2001.6551361x

Prosperini N, Perugini D (2008) Particle size distributions of some soils from the Umbria Region (Italy): Fractal analysis and numerical modelling. Geoderma 145: 185-195. https://doi.org/10.1016/j.geoderma.2008.03.004

Qi F, Zhang R, Liu X, et al. (2018) Soil particle size distribution characteristics of different land-use types in the Funiu mountainous region. Soil Till Res 184: 45-51. https://doi.org/10.1016/j.still.2018.06.011

Rényi A (1955) On a new axiomatic theory of probability. Acta Math Acad Sci Hungar 6: 285-335. https://doi.org/10.1007/bf02024393

Rodríguez-Lado L, Lado M (2017) Relation between soil forming factors and scaling properties of particle size distributions derived from multifractal analysis in topsoils from Galicia (NW Spain). Geoderma 287: 147-156. https://doi.org/10.1016/j.geoderma.2016.08.005

Rosemary F, Vitharana UWA, Indraratne SP, et al. (2017) Exploring the spatial variability of soil properties in an Alfisol soil catena. Catena 150: 53-61. https://doi.org/10.1016/j.catena.2016.10.017

San José Martínez F, Martín MA, Caniego FJ, et al. (2010) Multifractal analysis of discretized X-ray CT images for the characterization of soil macropore structures. Geoderma 156: 32-42. https://doi.org/10.1016/j.geoderma.2010.01.004

Su M, Ding G, Gao G, et al. (2018) Multi -fractal analysis of soil particle size distribution of Pinus sylvestris var．mongolica plantations in Hulunbeier sandy land. Journal of Arid Land Resources and Environment 32: 129-135. (In Chinese) https://doi.org/10.13448/j.cnki.jalre.2018.345

Sun C, Liu G, Xue S (2016) Natural succession of grassland on the Loess Plateau of China affects multifractal characteristics of soil particle-size distribution and soil nutrients. Ecol Res 31: 891-902. https://doi.org/10.1007/s11284-016-1399-y

Taguas FJ, Martı n MA, Perfect E (1999) Simulation and testing of self-similar structures for soil particle-size distributions using iterated function systems. Geoderma 88: 191-203. https://doi.org/10.1016/S0016-7061(98)00104-9

Trangmar BB, Yost RS, Uehara G, 1986. Application of Geostatistics to Spatial Studies of Soil Properties. In: Brady, N C (Ed.), Advances in Agronomy. Academic Press, pp. 45-94.

Tripathi R, Nayak AK, Shahid M, et al. (2015) Characterizing spatial variability of soil properties in salt affected coastal India using geostatistics and kriging. Arab J Geosci 8: 10693-10703. https://doi.org/10.1007/s12517-015-2003-4

Tyler SW, Wheatcraft SW (1992) Fractal Scaling of Soil Particle-Size Distributions: Analysis and Limitations. Soil Sci Soc Am J 56: 362-369. https://doi.org/10.2136/sssaj1992.03615995005600020005x

Wang J, Lu X, Feng Y, et al. (2018) Integrating multi-fractal theory and geo-statistics method to characterize the spatial variability of particle size distribution of minesoils. Geoderma 317: 39-46. https://doi.org/10.1016/j.geoderma.2017.12.027

Wang J, Zhang J, Feng Y (2019) Characterizing the spatial variability of soil particle size distribution in an underground coal mining area: An approach combining multi-fractal theory and geostatistics. Catena 176: 94-103. https://doi.org/10.1016/j.catena.2019.01.011

Xia J, Ren R, Chen Y, et al. (2020) Multifractal characteristics of soil particle distribution under different vegetation types in the Yellow River Delta chenier of China. Geoderma 368: 114311. https://doi.org/10.1016/j.geoderma.2020.114311

Xu G, Li Z, Li P (2013) Fractal features of soil particle-size distribution and total soil nitrogen distribution in a typical watershed in the source area of the middle Dan River, China. Catena 101: 17-23. https://doi.org/10.1016/j.catena.2012.09.013

Zhou P, Zhuang WH, Wen AB, et al. (2016) Fractal features of soil particle redistribution along sloping landscapes with hedge berms in the Three Gorges Reservoir Region of China. Soil Use Manage 32: 594-602. https://doi.org/10.1111/sum.12307